

# Sonochemical Deposition of Air-Stable Iron Nanoparticles on Monodispersed Carbon Spherules

V. G. Pol,<sup>†</sup> M. Motiei,<sup>†</sup> A. Gedanken,<sup>\*,†</sup> J. Calderon-Moreno,<sup>‡</sup> and Y. Mastai<sup>§</sup>

Department of Chemistry, Bar-Ilan University, Ramat-Gan, 52900 Israel, Materials and Structures Laboratory, Tokyo Institute of Technology, 4259, Nagatsuta, Midori-ku, 226-8503 Yokohama, Japan, and Max-Planck-Institute of Colloids and Interfaces, Colloid Chemistry, Forschungs Campus Golm, Am Mühlenberg, Haus 2, D-14424 Potsdam, Germany

Received September 6, 2002. Revised Manuscript Received December 12, 2002

A novel route was used to prepare “perfect spherical” monodispersed carbon with a smooth surface, which has a surface area of  $8 \text{ m}^2/\text{g}$ . Air-stable iron nanoparticles with an average size of  $\sim 10 \text{ nm}$  were deposited on the surface of preformed carbon spherules with the aid of power ultrasound. This coating was achieved by ultrasonic irradiation of a slurry of carbon spherules and  $\text{Fe}(\text{CO})_5$  in diphenylmethane for 90 min under an argon atmosphere. The as-prepared amorphous material was annealed in argon at  $700 \text{ }^\circ\text{C}$ , forming air-stable iron deposited on carbon spherules. The product was characterized by XRD, TEM, EDAX, BET surface area, HR-SEM, TGA, DSC, magnetic measurements, electron paramagnetic resonance, and Raman spectroscopy.

## Introduction

The discovery of “new forms of carbon”, for example, fullerenes and carbene-like one-dimensional structures,<sup>1,2</sup> has greatly promoted the investigation of carbonaceous materials. A classification of these spherical carbon structures has been recently proposed by Inagaki,<sup>3</sup> according to their nanometric texture, that is, concentric, radial, or random arrangement of carbon layers. Carbon spheres,<sup>4–6</sup> beads,<sup>7</sup> onions,<sup>8</sup> and hollow carbons<sup>9</sup> have been synthesized by very different processes. Accordingly, various applications have been intensively developed, of which we highlight nanodevices,<sup>10a</sup> energy storage,<sup>10b</sup> separation technology,<sup>10c</sup> and so forth, which are attracting much interest from carbon scientists worldwide. Enormous research was carried out on the deposition of a variety of metal particles onto ceramic substrates and magnetic colloids immobilized in a polymer matrix. In most of the experi-

ments silica and alumina were used as a substrate. Alumina, as well as silica, are dissolved<sup>10d</sup> at high pHs and the alumina is also attacked at very low pHs. In contrast, activated carbons are stable in both acid and basic media.

The sonochemical method is simple and it is operated at ambient conditions. It is also easy to control the particle size of the product by varying the concentration of the precursors in the solution.<sup>11a</sup> Power ultrasound effects chemical changes due to cavitation phenomena involving the formation, growth, and implosive collapse of bubbles in liquid.<sup>11b</sup> These phenomena have been exploited to prepare a variety of metals, oxides, and composite nanoparticles<sup>11c</sup> and have recently been extended to produce core–shell-type materials.<sup>11d</sup> In recent publications, we discussed how we uniformly deposited metallic silver<sup>11e</sup> nanoparticles on silica spheres and europium oxide nanolayer<sup>11f</sup> on titania by controlling experimental conditions with the aid of power ultrasound. Ultrasound-induced cavitations have also been used to coat nanosized nickel on alumina microspheres,<sup>11g</sup> and iron/iron oxide on silica,<sup>11h</sup> imparting a magnetic function to the particles.

Supported catalysts are of special interest, as they allow for the fine dispersion and stabilization of small metallic particles.<sup>12a</sup> They provide access to a much larger number of catalytically active atoms than in the

\* To whom correspondence should be addressed. Fax: +972-3-5351250. E-mail: gedanken@mail.biu.ac.il.

<sup>†</sup> Bar-Ilan University.

<sup>‡</sup> Tokyo Institute of Technology.

<sup>§</sup> Max-Planck-Institute of Colloids and Interfaces.

- (1) Tanuma, S.; Palmichenko, A. V. *J. Mater. Res.* **1995**, *10*, 1120.
- (2) Iijima, S. *Nature* **1991**, *354*, 56.
- (3) Inagaki, M. *Carbon* **1997**, *35*, 711.
- (4) Serp, P.; Feurer, R.; Kalck, Ph.; Kihn, Y.; Faria, J. L.; Figueiredo, J. L. *Carbon* **2001**, *39*, 621.
- (5) Wang, Q.; Li, H.; Chen, L. Q.; Huang, X. J. *Carbon* **2001**, *39*, 2211.
- (6) Washiyama, M.; Sakai, M.; Inagaki, M. *Carbon* **1988**, *26*, 303.
- (7) Inagaki, M.; Washiyama, M.; Sakai, M. *Carbon* **1988**, *26*, 169.
- (8) Tomita, S.; Sakurai, T.; Ohta, H.; Fujii, M.; Hayashi, S. *J. Chem. Phys.* **2001**, *114*, 17, 7477.
- (9) Sharon, M.; Mukhopadhyay, K.; Yase, K.; Ijima, S.; Ando, Y.; Zhao, X. *Carbon* **1998**, *36*, 507.
- (10) (a) Collins, P. G.; Zettl, A.; Bando, H.; Thess, A.; Smalley, R. E. *Science* **1998**, *278*, 100. (b) Che, G.; Lakshmi, B. B.; Fisher, E. R.; Martin, C. R. *Nature* **1998**, *393*, 346. (c) Shiflett, M. B.; Foley, H. C. *Science* **1999**, *285*, 1902. (d) *Catalyst Supports and Supported Catalysts*, Stiles, A. B., Ed; Butterworths: Boston, 1987; p 57.

(11) (a) Cao, X.; Koltypin, Yu.; Kataby, G.; Prozorov, R.; Gedanken, A. *J. Mater. Res.* **1995**, *10*, 2952. (b) Suslick, K. S., Ed. *Ultrasound: Its Chemical, Physical and Biological Effects*; VCH: New York, 1988. (c) Ramesh, S.; Minti, H.; Reisfeld, R.; Gedanken, A. *Opt. Mater.* **1999**, *13*, 67. (d) Dokoutchaev, A.; James, J. T.; Koene, S. C.; Pathak, S.; Prakash, G. K. S.; Thompson, M. E. *Chem. Mater.* **1999**, *11*, 2389. (e) Pol, V. G.; Srivastava, D. N.; Palchik, O.; Palchik, V.; Slifkin, M. A.; Weiss, A. M.; Gedanken, A. *Langmuir* **2002**, *18*, 3352. (f) Pol, V. G.; Reisfeld, R.; Gedanken, A. *Chem. Mater.* **2002**, *14*, 3920. (g) Zhong, Z.; Mastai, Y.; Koltypin, Y.; Zhao, Y.; Gedanken, A. *Chem. Mater.* **1999**, *11*, 2350. (h) Ramesh, S.; Prozorov, R.; Gedanken, A. *Chem. Mater.* **1997**, *9*, 546.

corresponding bulk metal. Recently, Li et al. used nongraphitic carbon spherules and pinned nanosized SnSb alloy<sup>12b</sup> particles on the surface of micrometer-sized hard carbon spherules by a coprecipitation method. This process was conducted in a glycol solution at low temperature and the product was used as anode materials for a lithium ion battery.

Coated magnetic nanoparticles may have important applications as materials for magnetic data storage, xerography, and magnetic resonance imaging.<sup>13a</sup> A protective layer on the surface of the particles prevents interaction between closely spaced magnetic bits and provides oxidation resistance.<sup>13b</sup> Coated, air-stable iron nanoparticles are of particular interest since iron has the highest magnetic moment among the ferromagnetic transition metals and is easily oxidized. There are a few reports in the literature on the synthesis of air-stable iron. For example, an iron catalyst prepared by high-temperature pyrolysis of tetraphenylporphyrins adsorbed on carbon black. The stability toward oxidation is achieved by coating the particles with a protective layer.<sup>13c</sup> Hayashi et al. studied the functional effects of carbon-coated<sup>13d</sup> iron metal particles for magnetic recording media. Recently, Nikitenko et al. synthesized highly magnetic, air-stable iron–iron carbide<sup>13e</sup> nanoparticles by using power ultrasound. To prepare air-stable iron nanoparticles, they conducted sonochemical decomposition of  $\text{Fe}(\text{CO}_5)$  in diphenylmethane (DPhM), an aromatic solvent. They revealed that sonolysis of neat DPhM forms a polymer-like solid product, which coats the surface of iron nanoparticles formed simultaneously from  $\text{Fe}(\text{CO}_5)$ . In this article, we report on a novel route to synthesize carbon spherules. These spherules are used as a substrate for the sonochemical deposition of air-stable iron on the surface. The sonochemical methods qualify for the deposition task due to their ability to combine the synthesis of air-stable magnetic particles and their deposition on a spherical carbon substrate in a single operation.

## Experimental Section

**Synthesis of Carbon Spherules.** The novel synthesis of carbon spherules was carried out by selecting Mesitylene [97%, 1,3,5-trimethylbenzene ( $\text{C}_6\text{H}_3(\text{CH}_3)_3$ ), Aldrich Chemical Co.] as a precursor. A 4-mL closed vessel cell was assembled from stainless steel swagelock parts. A  $1/2$ -in. union part was capped from both sides by a standard plug. For this synthesis, 2 mL of mesitylene was introduced into the cell at room temperature under air. The cell was placed inside an iron pipe at the center of the furnace and the temperature was raised at a heating rate of  $5\text{ }^\circ\text{C}/\text{min}$ . The closed vessel was heated at  $700\text{ }^\circ\text{C}$  for 3 h. The reaction took place at the autogenic pressure of the precursor. The cell was gradually cooled to room temperature and opened and a dark black powder was collected. The

morphology of the formed monodispersed carbon spherules was observed by transmission and a scanning electron microscope.

**Sonochemical Deposition of Iron Nanoparticles on Carbon Spherules.** The sonochemical deposition of air-stable iron nanoparticles on carbon spherules was carried out using the following procedure. Diphenylmethane (>99%, Fluka) and  $\text{Fe}(\text{CO})_5$  (97%, Aldrich) were used without additional purification. The pre-prepared 1 g of carbon spherules and 0.3 mL of  $\text{Fe}(\text{CO})_5$  were added to 100 mL of diphenylmethane in a sonication cell, and the cell was attached to the sonicator horn under flowing argon. The sonication of the slurry with the high-intensity ultrasound irradiation was carried out for 90 min by direct immersion of the titanium horn (Sonics and Materials VCX 600 sonifier, 20 kHz, 40 W/cm<sup>2</sup>) in a sonication cell, under a flow of argon gas. During sonication, the color of the solution changed rapidly from yellow to black. Temperature during sonication was kept at  $30\text{ }^\circ\text{C}$ . The black solid product was removed by centrifugation at 9000 rpm, washed once with toluene and twice with dry pentane inside a  $\text{N}_2$ -filled glovebox, and dried under vacuum at room temperature for 8 h. The vacuum-dried product was termed as an “as-prepared” sample. The crystallization of the as-prepared solid products obtained from sonication was carried out by heating a small amount of the sample in a quartz tube at  $700\text{ }^\circ\text{C}$  under flowing argon gas for 3 h.

**Characterization.** The X-ray diffraction patterns of the products were measured with a Bruker AXS D\* Advance Powder X-ray diffractometer (using  $\text{Cu K}\alpha = 1.5418$  radiation). High-resolution scanning electron microscope (HR-SEM) images were obtained using JEOL 6300F. The elemental composition of the material was analyzed by energy-dispersive X-ray analysis (Kevex). The particle morphology and the nature of its adherence to carbon spherules were studied with transmission electron microscopy, which was done on a Zeiss EM 912 OMEGA operating at an acceleration voltage of 120 kV. One drop of the suspension samples was applied to a carbon-coated 400-mesh copper grid and left to dry in air. The dry powder of carbon spherules was also immersed in epoxy plastic (according to Spurr’s formulation) and put into a capsule to harden. The LKB Ultatome III with a diamond knife used to cut hard carbon spheres and ultrathin sections were mounted on uncoated 400-mesh copper grids. The Brunauer–Emmett–Teller (BET) surface area measurements were performed by a Micromeritics (Gemini 2375) analyzer. Thermogravimetric analysis was carried out under a stream of nitrogen, at a heating rate of  $3\text{ }^\circ\text{C}/\text{min}$  using a Mettler TGA/STDA 851. Differential scanning calorimetric (DSC) analysis of the sample in a crimped aluminum crucible was carried out up to a temperature of  $550\text{ }^\circ\text{C}$ , using a Mettler DSC-301 under a stream of nitrogen, at a heating rate of  $3\text{ }^\circ\text{C}/\text{min}$ . The magnetic measurements were performed on a vibrating sample magnetometer (VSM-Oxford-3001). Electron paramagnetic resonance (EPR) spectra were recorded on a Bruker EPR spectrometer (ER083 CS) operating at X-band ( $v = 9.77\text{ GHz}$ ), with a 100-kHz magnetic field modulation. A standard Renishaw Raman spectrometer was employed, using the 514.5-nm line of an Ar laser as the excitation source.

## Results and Discussion

**Electron Microscopy Studies.** Figure 1a shows the scanning electron micrograph of micrometer-size carbon spherules synthesized by using mesitylene as a precursor for the first time. The carbon spherules have a narrow size distribution, with their diameter in the range of  $2.4\text{--}2.5\text{ }\mu\text{m}$ . The SEM micrograph of carbon spherules taken at high resolution (Figure 1b) showed that their surface is smooth and completely spherical in shape. To clarify whether these spherules are solid or hollow, we took a horizontal cross section out of a spherule during TEM measurements, as mentioned in the characterization section. It was clearly seen that the

(12) (a) Auer, E.; Freund, A.; Pietsch, J.; Tacke, T. *Appl. Catal.*, **1998**, *173*, 259. (b) Li, H.; Wang, Q.; Shi, L. H.; Chen, L. Q.; Huang, X. *J. Chem. Mater.*, **2002**, *14*, 103.

(13) (a) Harris, P. J. F. *Carbon Nanotubes and Related Structures*, Cambridge University Press: New York, 1999. (b) Jiao, J.; Wang, S. X.; Withers, J. C. *J. Appl. Phys.*, **1996**, *80*, 103. (c) Faubert, G.; Cote, R.; Guay, D.; Dodelet, J. P.; Denes, G.; Bertrand, P. *Electrochim. Acta*, **1998**, *43*, 341. (d) Hayashi, K.; Ohsugi, M.; Kamigaki, M.; Xia, B.; Okuyama, K. *Electrochim. Solid State Lett.*, **2002**, *5*, J9. (e) Nikitenko, S. I.; Koltypin, Y.; Palchik, O.; Felner, I.; Xu, X. N.; Gedanken, A. *Angew. Chem., Int. Ed.*, **2001**, *40*, 4447. (f) Cannas, C.; Concias, G.; Gatteschi, D.; Musinu, A.; Piccaluga, G.; Sangregorio, C. *J. Mater. Chem.*, **2002**, *12*, 3141.

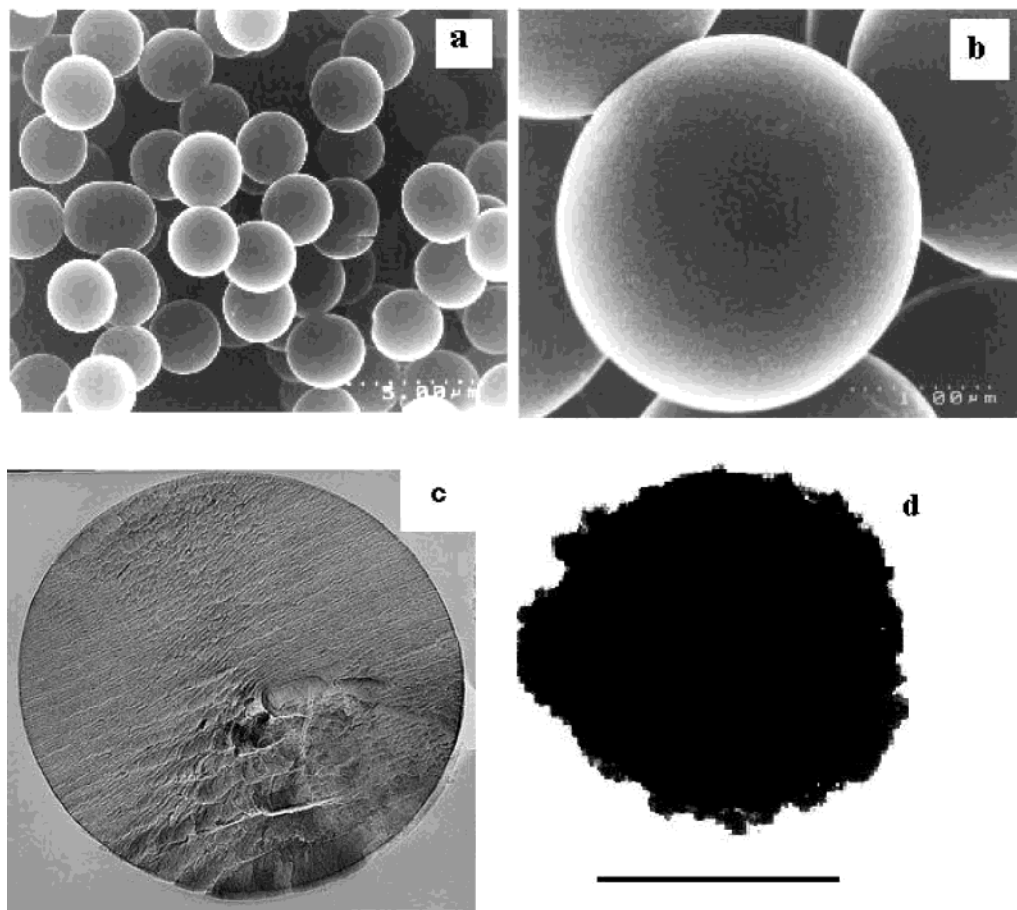


**Figure 1.** Scanning electron micrographs of (a) monodispersed carbon spherules, (b) single carbon spherule at high resolution (bar indicates 1  $\mu\text{m}$ ), (c) TEM of horizontal cross section of the carbon spherule; (d) TEM of iron nanoparticles deposited on the carbon spherules (bar indicates 2  $\mu\text{m}$ ).

spherules are solid or full (Figure 1c). To check the stress/strain, we applied 4000-psi pressure on these carbon spherules for 20 min. It was revealed that under this pressure no changes in the size or shape of the spherules are observed by TEM measurements. This also indicates as to the solid nature of the spherules. Thus, we conclude that the formed spherules are solid and not hollow.

TEM was used to study the iron nanoparticle morphology and the nature of its adherence to the carbon spherules. Our first experiments involved the attempt to deposit noble metals such as Pt, Au, and Ag on the surface of carbon spherules. It was found that, unlike the smooth deposition of Au and Ag<sup>11e</sup> on silica spheres, it is difficult to deposit these nanoparticles on the surface of carbon spherules under a sonochemical method. On the other hand, our attempts to deposit a variety of magnetic nanoparticles such as iron, nickel, and cobalt on the surface of spherules were successful. In this article, we present the results related to iron nanoparticle deposition on the carbon spherules. In our attempt to deposit Ag, we followed our previous report.<sup>11e</sup> Uncoated agglomerates with tubular morphology of silver particles are observed in TEM measurements. During the platinum deposition, hydrogen hexachloroplatinate(IV) was used as a platinum precursor. This precursor was reduced under the atmosphere of a hydrogen:argon (5:95%) atmosphere, keeping all other experimental conditions the same. Only a few of the

platinum nanoparticles ( $\sim$ 8-nm size) were deposited on the surface of the spherules. These particles also have the tendency to agglomerate, maybe due to the sonopolymer coated on the surface of platinum nanoparticles. The TEM picture in Figure 1d demonstrated the adherence of iron nanoparticles to the surface of the carbon spherule. Most of the deposited iron nanoparticles have a diameter of approximately  $\sim$ 10 nm and they completely cover the surface of the carbon spherules. Both the amorphous and annealed (700  $^{\circ}\text{C}$ /3 h) samples of iron deposited on carbon spherules showed a tendency toward agglomeration.

**X-ray Diffraction Measurements.** In Figure 2a, the X-ray diffraction patterns of the as-prepared material of iron nanoparticles deposited on carbon spherules are shown. The amorphous nature of the products is demonstrated by the absence of any diffraction peaks. An air-stable, dark black magnetic powder is formed after annealing of the as-prepared sample at 700  $^{\circ}\text{C}$ , in an Ar atmosphere. The XRD pattern for the annealed sample is shown in Figure 2b. It indicates a body-centered cubic phase of metallic iron (PDF: 6-696). The peaks at  $2\Theta = 44.67^{\circ}$  and  $65.02^{\circ}$  are respectively assigned as 110 and 200 diffraction lines of bcc Fe particles. In addition, very small peaks were observed, which are assigned to Fe<sub>3</sub>C. The carbon/Fe<sub>3</sub>C-coated iron nanoparticles deposited on carbon spherules exhibit strong resistance to oxidation, evidenced by the lack of an oxide peak. The high stability of the deposited

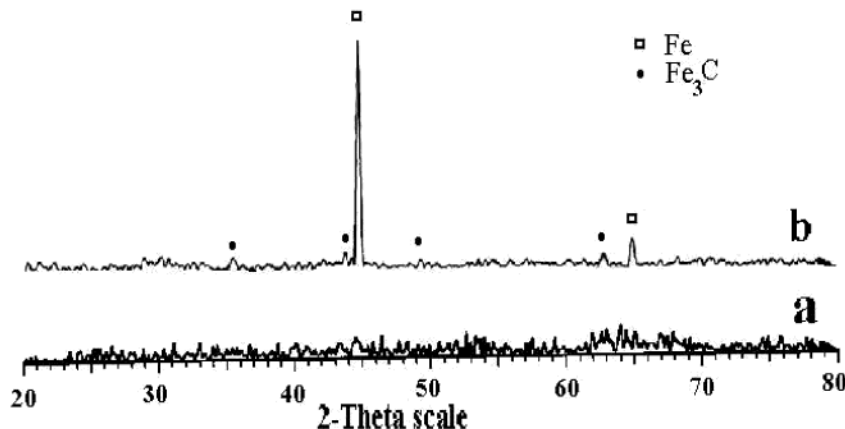


**Figure 2.** X-ray diffraction patterns of (a) an as-prepared sample of iron nanoparticles deposited on the carbon spherules and (b) an annealed sample of iron nanoparticles deposited on the carbon spherules.

nanoparticles could be related to the protective shell formed on the surface. The annealed sample of deposited iron nanoparticles is stable in an air atmosphere, as confirmed by XRD a month after the synthesis.

The elemental composition of the carbon spherules and deposited material was analyzed by energy-dispersive X-ray analysis. In the sample of carbon spherules only carbon was observed, and no evidence was found for any other impurity. The iron nanoparticle sample deposited on carbon spherules showed the presence of iron and carbon. The iron content in this sample was about 7 wt %. This value is close to the molar ratio of  $\text{Fe}(\text{CO}_5)/\text{carbon spherules}$  in the starting solution.

The measured BET surface area of smooth monodispersed carbon spherules was  $8 \text{ m}^2/\text{g}$ . After deposition of air-stable iron nanoparticles on the surface of carbon spherules by a sonication method, the surface area changed drastically. The as-prepared material shows a surface area of  $34 \text{ m}^2/\text{g}$ . The sample annealed at  $700^\circ\text{C}$  for 3 h shows a surface area of  $30 \text{ m}^2/\text{g}$ . Wang et al. synthesized carbon spherules, selecting sugar as a precursor<sup>5</sup> with uniform nanopores of about  $0.4 \text{ nm}$  in diameter, which has a BET surface area of  $400 \text{ m}^2/\text{g}$ . They found that  $\text{H}_2\text{O}$ ,  $\text{CO}$ , and  $\text{CO}_2$  were mostly released from the sample. The extraction of  $\text{H}$ ,  $\text{O}$ , and  $\text{C}$  gives rise to large quantities of micropores throughout the bulk of the samples. They proposed that, at high pressure and temperature, the escape of water through the flexible dewatering sugar played an important role in the construction of the microporous structure. The calculated surface area for  $2.5\text{-}\mu\text{m}$  carbon spherules is  $1.076 \text{ m}^2/\text{g}$ , considering the density of carbon as  $2.23 \text{ g}/\text{cm}^3$ . If the density of the carbon spherules is taken as  $1.5 \text{ g}/\text{cm}^3$ , a surface area of  $1.60 \text{ m}^2/\text{g}$  is calculated for the spherules. We have measured a surface area of  $8 \text{ m}^2/\text{g}$  for the  $2.5\text{-}\mu\text{m}$  carbon spherules. The measured surface area is larger than the calculated value by a factor of at least 5. This can be explained by assuming the existence of some small pores on the surface. The pores can result from the reaction of hydrogen and oxygen which yield water, which helps in the formation of very small micropores.<sup>5</sup> However, unlike the previous case,<sup>5</sup> where a surface area of  $400 \text{ m}^2/\text{g}$  is obtained, the amount of oxygen in our swagelock is very small, leading to a much smaller amount of water and a smaller surface area. A more favorable explanation can be that, on the nanometer scale, the surface is not as

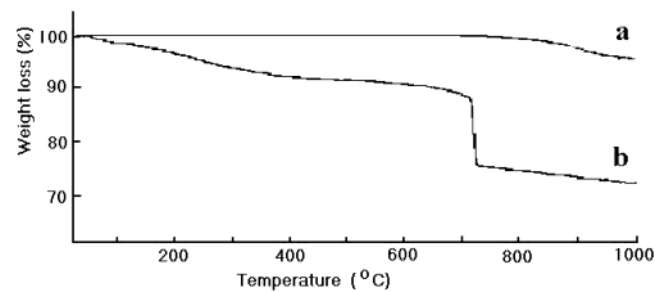


**Figure 3.** Thermogravimetric analysis (TGA) profiles of (a) carbon spherules and (b) an as-prepared sample of iron nanoparticles deposited on the carbon spherules.

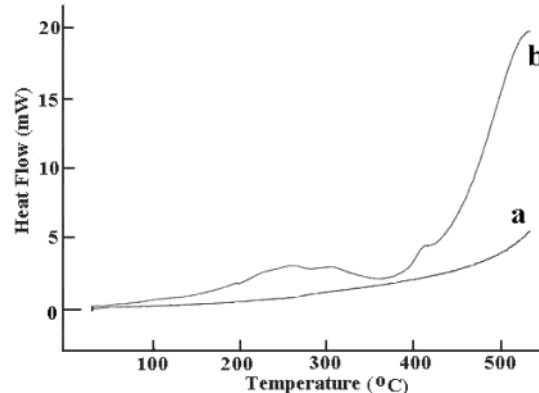


**Figure 4.** Differential scanning calorimetric curves for (a) carbon spherules and (b) an as-prepared sample of iron nanoparticles deposited on the carbon spherules.

smooth as that observed in the low-resolution TEM and HR-SEM. High-resolution TEM pictures demonstrate that the surface is not flat and consists of small hills and valleys that increase its surface area.

**Thermal Properties.** The TGA curves of the substrate carbon spherules and the as-prepared sample of iron coated on the carbon spherules are shown in (a) and (b), respectively, of Figure 3. The bare carbon spherules showed a total weight loss of 5%, against a 30% loss for the iron-coated sample. The weight loss demands an understanding of the nature of thermally desorbable species on the surface of iron or carbon spherules. The as-prepared sample showed a three-step weight loss in the temperature region of  $40\text{--}1000^\circ\text{C}$ . The first step weight loss, around 10% in the wide temperature range of  $40\text{--}600^\circ\text{C}$ , can be associated with

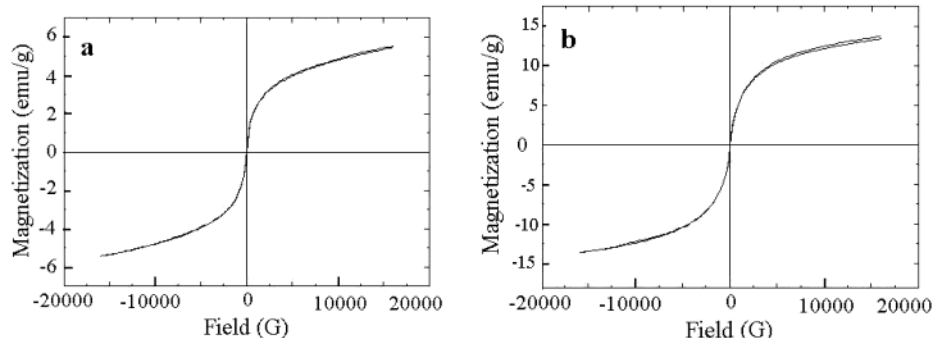


**Figure 5.** Room-temperature magnetization curves for (a) an as-prepared sample of iron nanoparticles deposited on the carbon spherules and (b) an annealed sample of carbon spherules deposited with iron nanoparticles.

the loss of carbon and hydrogen, which was formed on the surface of iron or carbon spherules during sonolytic decomposition products of diphenylmethane.<sup>13e</sup> This loss might also contain some nonpolymerized solvent. The second step of weight loss, around 15% in the temperature range of 600–750 °C, could be associated with complete decomposition of C–H bonds and the release of H<sub>2</sub>. In the third step, a temperature range of 750–950 °C, 5% weight loss, was observed in both carbon spherules as well as in the iron-coated sample.

Parts (a) and (b) of Figure 4 show the DSC curves for the carbon spherules and the as-prepared sample of iron nanoparticles deposited on carbon spherules, respectively. The DSC curve obtained for carbon spherules was featureless (Figure 4a). The DSC curve obtained for iron deposited on a spherule sample showed two exothermic peaks obtained at ~250 °C (broad) and 420 °C (small). The exothermic peak at 250 °C is related to the crystallization of the amorphous iron. Indeed, after cooling and a second heating cycle, the DSC spectrum was featureless (data not shown).

**Magnetic Measurements.** The magnetic properties were investigated by magnetic susceptibility and by the electron spin resonance (ESR) method, as outlined in the Experimental Section. The magnetization loops for the as-prepared and annealed samples of iron deposited on carbon spherules are presented in (a) and (b) of Figure 5. The magnetization does not saturate at 16 K G and does not show hysteresis. On the basis of these results, we conclude that the particles are superparamagnetic. This is not surprising since iron particles smaller than 14 nm are expected to be superparamagnetic.<sup>13f</sup> The saturation magnetizations “Ms” for the as-prepared and annealed samples are 6 and 14 emu g<sup>-1</sup>, respectively. The reported values for such a type of air-stable iron<sup>13e</sup> and for the bcc Fe given in the literature<sup>14a</sup> are 212 and 222 emu g<sup>-1</sup>, respectively. Taking into account the weight of iron (7 wt %) present in the entire material (from EDAX), the saturation magnetization of an annealed sample of iron deposited on carbon spherules works out to approximately 200 emu g<sup>-1</sup>.

Electron paramagnetic resonance is a powerful technique for studying the microstructure and the electronic properties of carbon or related materials. The resonance

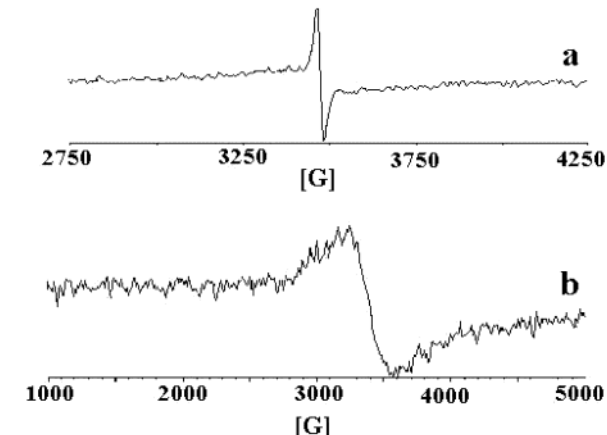


**Figure 6.** Electron paramagnetic resonance (EPR) exhibited at room temperature by (a) carbon spherules and (b) an as-prepared sample of iron nanoparticles deposited on the carbon spherules.

spectrum of a bare carbon spherule sample taken at room temperature is shown in Figure 6a. The *g* factor is a dimensionless constant and is equal to 2.002319 for the unbound electron.<sup>14b</sup> The exact value of the *g* factor reflects the chemical environment, particularly when heteroatoms are involved, because the orbital angular momentum of the electron can have an effect on the value of the transition  $\Delta M_s = \pm 1$ . The carbon spherule sample showed a peak-to-peak separation ( $\Delta H_{pp}$ ) of 40 G and a *g* value 2.00277. A sharp and narrower paramagnetic resonance signal (width 40 G) can be associated with the paramagnetic nature of the carbon spherules. The experimental *g* value of 2.00277 for these particles is in good agreement with a value of 2.0028 reported<sup>15a</sup> for carbon nanostructures.

Figure 6b shows the resonance spectrum of iron nanoparticles deposited on a carbon spherule sample. The as-prepared sample exhibits a peak-to-peak separation ( $\Delta H_{pp}$ ) of 250 G and a *g* value of 1.98, which is typical for an Fe<sub>2</sub>O<sub>3</sub>-capped particle.<sup>15b</sup> The broadening of the ESR line arises from strong interparticle dipolar interactions that provide an effective spin relaxation mechanism.<sup>15b</sup> The crystalline annealed sample was highly magnetic and a resonance spectrum could not be recorded under identical conditions, even with small amounts of the sample measured.

(14) (a) *Metals Handbook*, 9th ed.; American Society for Metals: Metal Park, OH, 1985; Vol. 9 (Metallurgy and Microstructures). (b) Willard, H. H.; Merritt, L. L., Jr.; Dean, J. A. *Instrumental Methods of Analysis*, 5th ed.; Van Nostrand: New York, 1974.

(15) (a) Bandow, S. *J. Appl. Phys.* **1996**, *80*, 1020. (b) Sharma, V. K.; Waldner, F. *J. Appl. Phys.* **1977**, *48*, 4298.

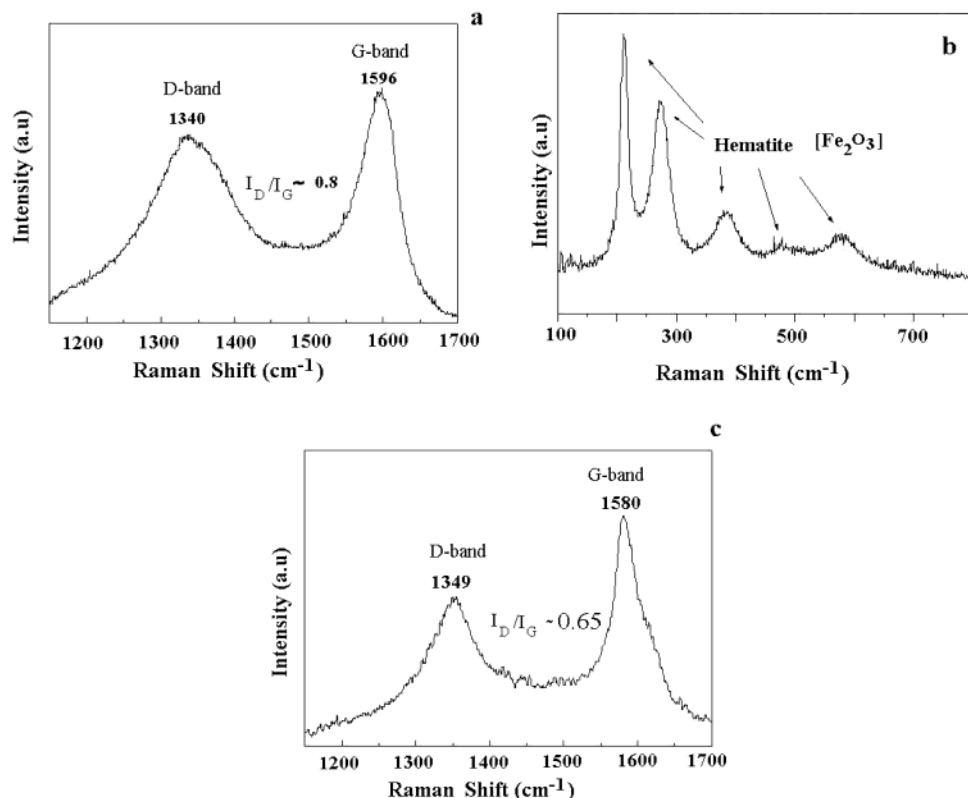


**Figure 7.** Raman spectra of (a) carbon spherules, (b) an as-prepared sample of iron nanoparticles deposited on the carbon spherules, and (c) an annealed sample of iron nanoparticles deposited on the carbon spherules.

**Raman Spectroscopy.** The Micro-Raman spectrum of the bare carbon spherules is shown in Figure 7a. The D- and G-bands of graphitic carbon show an intensity ratio: of  $I_D/I_G = 0.8$  in the bare carbon spherules. This ratio indicates an amorphous carbon structure, with a high content of lattice edges or plane defects within the analyzed spherule.<sup>16a</sup> Micro-Raman analysis of the amorphous product, which was not anchored to the carbon spherules, was carried out and revealed peaks corresponding to hematite ( $\text{Fe}_2\text{O}_3$ ),<sup>16b,16c</sup> as shown in Figure 7b. The hematite was formed by local oxidation of the mainly amorphous iron matrix (the sample was not annealed). However, XRD analysis did not detect any crystalline phase after sonochemical deposition. The peaks are detected only in a micro-Raman mode over small analyzed areas ( $\sim 1\text{--}2 \mu\text{m}$ ), explaining why no crystalline phase could be detected in the bulk sample by XRD.

The micro-Raman measurements on single spherules did not reveal the presence of haematite after thermal annealing (Figure 7c). The G-band shifts toward lower frequencies, typical of more ordered graphitic carbon, while the D-band shifts to higher frequencies. The relative intensity ratio of the disorder-associated D-band is reduced significantly compared with the increased intensity of the G-peak associated with graphitic carbon. The Raman results indicate that the most disordered part of the carbon outer surface, C atoms with

so-called dangling bonds (defects in the graphitic lattice), tend to disappear during sonochemical deposition. During the sonochemical treatment, thermal effects caused by the high local temperatures in the spherule's surface, and preferential etching of more reactive disordered carbon, result in a more graphitic-like alignment of the lattice planes in the coated carbon spherules.

**Proposed Mechanism.** After the collapse of the bubbles near solid surfaces of liquid powder, slurries, microjets, and shock waves are created, which can accelerate the iron nanoparticles to move at very high velocities<sup>17</sup> toward the surface of carbon spherules. These microjets accelerate the solid iron nanoparticles to very high speeds, and thus lead to sintering of the particles to the carbon surface. When the slurry of carbon spherules and iron pentacarbonyl in diphenyl methane is sonicated, the iron nanoparticles formed are thrown at the surfaces of the carbon spherules, causing the carbon surface to melt and dissolve in iron. This happens only with iron and does not happen with silver, gold, and platinum. Carbon does not dissolve in these metals and does not form an alloy with them. If this explanation is correct, we predict that Cr, which is also known to form an alloy with carbon, will be a good candidate for coating on the carbon spherules. Due to the orientation of these ultrasonic microjets, the very short lifetime (microseconds) of cavitation bubbles,<sup>17,11b</sup> and a possible interparticle collision between iron and carbon spherules, causes a change in surface morphology and reactivity,<sup>17</sup> which finally results in binding or nanodeposition of iron.

(16) (a) Dresselhaus, M. S.; Dresselhaus, G.; Pimenta, M. A. In *Analytical Application of Raman Spectroscopy*; Pelletier, M. J., Ed.; Blackwell Science: Oxford, 1999; Chapter 9. (b) Batonneau, Y.; Laureyns, J.; Merlin, J.-C.; Claude, B. *Anal. Chim. Acta* **2001**, *446*, 23. (c) Lucia, B.; Robin, J.; Clark, H. *Spectrochim. Acta, Part A* **2001**, *57*, 1491.

(17) Doktycz, S. J.; Suslick, K. S. *Science* **1990**, *247*, 1067.

### Conclusions

This paper has concentrated on the coating of micrometer-sized carbon spherules and has not touched on the question of the mechanism by which they are formed. This mechanism is now under study. The carbon spherules, which served as the substrate for the coating, were prepared by using mesitylene as a precursor. Mesitylene undergoes thermal decomposition, yielding the carbon spherules and, most probably, hydrogen molecules. The carbon spherules have a diameter of 2.5  $\mu\text{m}$  and a narrow size distribution, and they show a BET surface area of 8  $\text{m}^2/\text{g}$ . The paramagnetic nature of the carbon spherules was evidenced by a sharp and narrow paramagnetic resonance signal of ESR. For the first time air-stable iron nanoparticles with an average size of  $\sim 10$  nm were deposited on the surface of preformed carbon spherules with the aid of power ultrasound. The

high saturation magnetization of an annealed sample of iron deposited on carbon spherules works out to 200 emu  $\text{g}^{-1}$ . ESR and Raman measurements revealed that only the as-prepared sample could undergo local oxidation of amorphous iron. On the other hand, the annealed sample cannot be oxidized at ambient conditions. This is evidenced from the XRD measurement showing only bcc Fe and very small peaks of  $\text{Fe}_3\text{C}$ , after the product stood for a long time in the open air.

**Acknowledgment.** V. G. Pol is grateful to the President's Fund of Bar-Ilan University, Israel, for financial assistance. A. Gedanken thanks the DIP Organization (Deutsche-Israeli Projects) for their financial help administered by the BHSF, Germany.

CM020898M